DIELECTRIC-LINED CIRCULAR DEFLECTORS FOR ULTRAHIGH-ENERGY BEAM SEPARATORS*

C. T. M. Chang
Argonne National Laboratory
Argonne, Illinois

Summary

Circular deflectors lined with boron nitride, beryllia, and alumina are studied for application to ultrahigh-energy beam separators. These deflectors are designed at an aperture of 1 cm^2 at 5.6 and 8.5 GHz. The attenuation length, transverse shunt impedance, and group velocity are presented in graphs.

Introduction

In the last few years, there was considerable interest in the design and development of CW separated beams for counter experiments at energy in excess of 40 GeV.[1,2] Among the various beams considered, the use of superconducting iris-loaded deflectors provide an ideal solution for these applications. Unfortunately, the progress in the fabrication and construction of superconducting deflectors has not been sufficient to ensure a stable operation in the near future. A normal RF separator using series of iris-loaded deflectors was proposed by Foelsche as an interim convention option.[1] Another alternative scheme was proposed by Sandweiss in which the partially dielectric-loaded deflectors were used.[2] However, unlike the well-known iris-loaded counterparts, the dielectric-loaded deflectors were not studied until recently,[3-6] and their properties are still foreign to many beam designers. In an earlier report,[7] Kustom presented a study of dielectric-loaded rectangular deflectors for high-energy beams. This note provides a similar discussion into the properties of dielectric-lined circular deflectors for ultrahigh-energy beams, so that various kinds of deflectors can be compared intelligently.

General Considerations

As shown in Fig. 1, the deflector under consideration is a circular waveguide, alternately filled with two kinds of disks of relative dielectric constants ϵ_1 and ϵ_2 and thicknesses t_1 and t_2, respectively. To simplify our study, let $\epsilon_1 = 1$ (free space) and ϵ_r be that of boron nitride, beryllia, or alumina. All of them have relatively low RF loss, adequate thermal conductivity, and high-vacuum properties. Table I lists the relative dielectric constant, ϵ_r, loss tangent, δ, and thermal conductivity, K_d, of these materials. The beam aperture $A (\equiv \pi a^2)$ is chosen to be 1 cm^2, deemed to be adequate for these beams. The phase velocity, V_{ph}, of the deflecting (HEM_{11}) mode of these deflectors is set at c (the velocity of light in free space), which is, for all practical purpose, equal to that of the ultrahigh-energy particles. By operating at $V_{ph} = c$, the deflecting force in a dielectric-lined deflector becomes exactly uniform over the entire aperture. The operating frequency, f_o, is chosen at X-band to keep the drift space for 2π phase slip between the wanted and unwanted particles at a tolerable limit. The specific frequency of 8.5 GHz is chosen to correspond to that of a high-power tube, which is commercially available. With the above condition, one can calculate b for a given dielectric with changing r $[\equiv t_1/(t_1 + t_2)]$. Curves 1, 2, and 3 of Fig. 2 show the ratio b/a of three groups of deflectors calculated at 8.5 GHz for boron nitride, beryllia, and alumina linings, respectively. Curve 4 of Fig. 2 is calculated at 5.6 GHz with boron nitride linings. It is easily seen that the thickness of the dielectric lining is increased to make up the loss of dielectric materials due to the increase of r, so that the operating conditions are maintained at $V_{ph} = c$ and $f_o = 8.5$ GHz (5.6 GHz for curve 4). Note that isotropically lined deflectors are represented by the case at $r = 0$.

Properties of the Dielectric-Lined Circular Deflectors

Since it is always desirable to operate deflectors in the range where only a single mode can propagate, the cutoff frequencies of the deflectors defined by b's given in Fig. 2 are calculated. One finds that the beryllia- and alumina-lined deflectors do not become degenerate until $r \gtrsim 0.7$. However, for the boron nitride-lined deflectors defined by curve 1 of Fig. 2, the cutoff of TM_{01} mode is always below 8.5 GHz. Thus special attention is required to ensure that no TM_{01} mode will be excited if these deflectors are used. An alternative way is to operate at 5.6 GHz (defined by curve 4 of Fig. 2), so that the TM_{01} modes do not propagate in structures with $r < 0.475$ at the operating frequency.

With the operating conditions and the dimensions of the groups of deflectors defined, a study of the traditional figures of merit is now in order. (i) Attenuation Length, $1/\alpha$; Attenuations of RF power in a dielectric-lined deflector are contributed by the wall loss and the dielectric loss. These losses decrease for structures with larger r. The decrease of the former is due to the lower wall-current densities resulted from larger physical sizes of the deflectors. The decrease of the latter is a result of the presence of less lossy material inside these deflector structures. Our calculation shows that for both boron nitride and alumina structures, wall loss is the major contributor to the attenuation. However, the relatively large loss tangent has made the contribution of dielectric loss in the group of beryllia deflectors comparable to those of wall loss. Figure 3 presents the combined attenuation of these deflectors in terms of the attenuation length. They are generally very long compared with their iris-loaded counterparts. The label on each curve here, as well as in all the subsequent figures, signifies that it

* Work performed under the auspices of the U.S. Atomic Energy Commission.

represents the characteristic curve of the group of structures defined by the curve with the same label given in Fig. 2. (ii) Transverse Shunt Impedance, R_{ts}; Since $R_{ts} \equiv E_0^2/(2\alpha P)$, where E_0 is the equivalent deflecting field and P is the input power, the transverse shunt impedance is used to measure the effectiveness of a given deflector. Figure 4 presents several E_0 - r curves calculated with 0.5 MW input power. Figure 5 shows the corresponding R_{ts}-r curves. The peak and dips in curves 2 and 3 are caused by the relatively slow variations in E_0 near r = 0.5. Typically, a 25-m-long deflector, operating from a matched 0.5 MW source and terminated into a matched load, is capable of giving 7 - 10 MeV/c transverse momentum to an ultrahigh-energy beam. (iii) Group Velocity, V_g; Since the V_{ph} - f curve for the deflecting mode of a dielectric-lined deflector is continuous, any change in V_{ph} can be compensated by a corresponding change of operating frequency. This relation is given by

$$\frac{\Delta V_{ph}}{c} = -\left[\frac{c}{V_g} - 1\right]\frac{\Delta f}{f_o} .$$

Thus for structures with larger V_g, the required Δf to restore a given change in V_{ph} is smaller. Figure 6 shows the V_g - r curves for the groups of structures defined in Fig. 2. They are positive (forward wave) and are relatively large in comparison with their iris-loaded counterparts.

To understand the tolerance problem in the construction of these deflectors, the dimensions and dielectric constant of the isotropic boron nitride-lined deflector operated at 5.6 GHz were changed simultaneously (from a to $a \pm \Delta$, b to $b \mp \Delta$, and ϵ_r to $\epsilon_r \mp \Delta\epsilon_r$, where Δ = 1 mil and ϵ_r = 0.01) to yield to the worst possible ΔV_{ph}. Thus ΔV_{ph} is approximately 0.01 c, which corresponds to Δf of less than 40 MHz.

With the above considerations, we conclude that an isotropically lined deflector operates more efficiently at low ϵ_r. However, as ϵ_r becomes larger, the anisotropically lined deflectors can be used to reduce losses. With r = 0 for boron nitride structures, r = 0.6 for beryllia structures, and r = 0.8 for alumina structures, the maximum radial fields of all four structures are, for 0.5 MW input, less than 2 MV/m. By assuming a uniform heat distribution inside the dielectric, one obtains temperature rises of about 20° C in the dielectrics for all four structures with the same input power.

TABLE I

	ϵ_r	$\delta \times 10^4$	K_d $\frac{kW - m}{m^2 - {}^oK}$
Boron Nitride	3.01	0.6	0.0188
Beryllia	6.5	3.0	0.247
Alumina	9.96	0.48	0.0368

References

1) H. Foelsche, NAL 1969 Summer Study, Vol. 1, (Batavia, Ill. 1969), pp. 119-124.

2) J. Sandweiss, NAL 1969 Summer Study, Vol. 1, (Batavia, Ill. 1969), pp. 125-131.

3) C. T. M. Chang, J. W. Dawson, and R. L. Kustom, IEEE Trans., NS-16, No. 3, 526 (1969).

4) C. T. M. Chang and J. W. Dawson, J. Appl. Phys. 41, 4493 (1970).

5) H. Hahn, Z. Angew Phys. 29, No. 5, 318 (1970).

6) C. T. M. Chang, IEEE Trans., MTT-20, 517 (1972).

7) R. L. Kustom, unpublished.

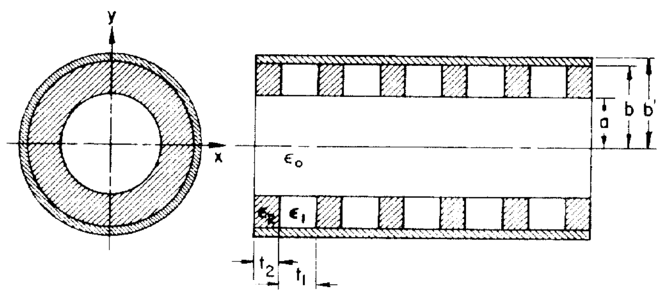

Fig. 1. Geometry of the dielectric-lined circular deflector.

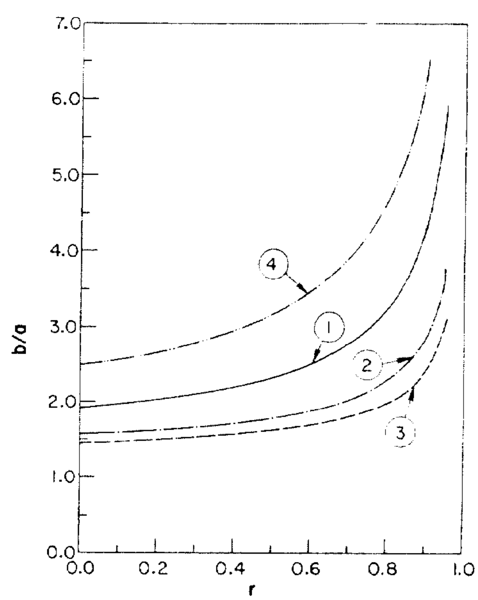

Fig. 2. Curves of outer radius b versus r $[\equiv t_1/(t_1 + t_2)]$. Curves 1, 2, and 3 are designed at V_{ph} = c and 8.5 GHz with boron nitride, beryllia, and alumina linings, respectively. Curve 4 is designed at V_{ph} = c and 5.6 GHz with boron nitride lining.

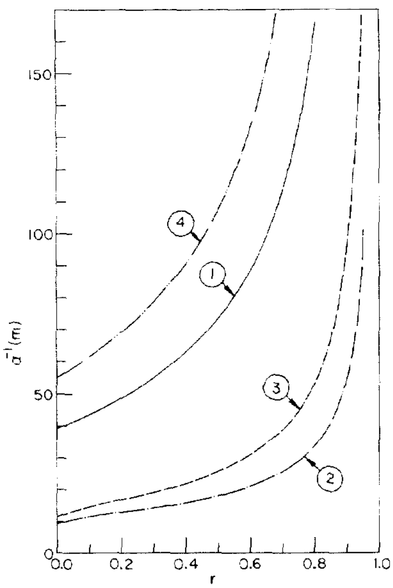

Fig. 3. Attenuation length α^{-1} versus r curves.

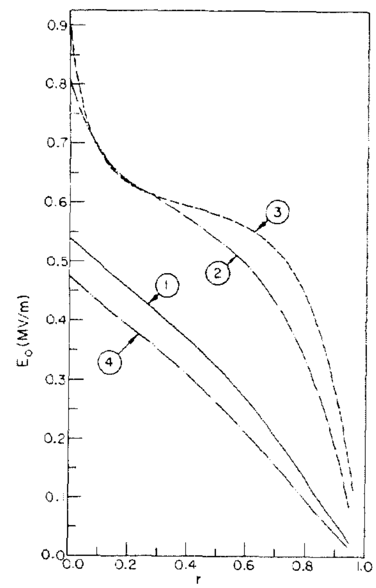

Fig. 4. Equivalent deflecting field E_o versus r curves. The fields are calculated at 0.5 MW input.

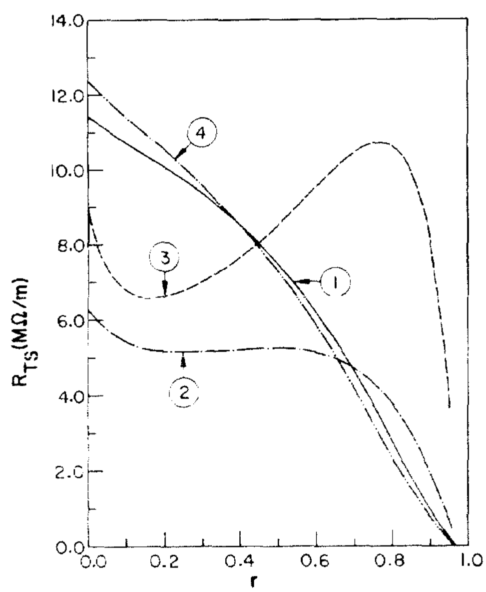

Fig. 5. Transverse shunt impedance R_{ts} versus r curves.

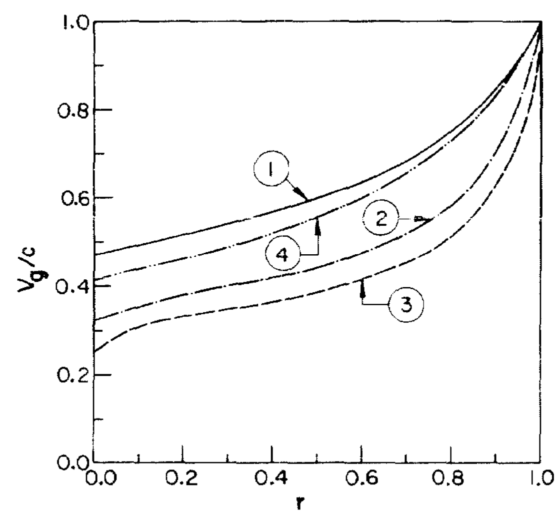

Fig. 6. Group velocity V_g versus r curves.